energies

MDPI

Article

Low-Temperature Hydrothermal Treatment (HTT) Improves the Combustion Properties of Short-Rotation Coppice Willow Wood by Reducing Emission Precursors

Sebastian Paczkowski [1,*], Victoria Knappe [2], Marta Paczkowska [1], Luis Alonzo Diaz Robles [3], Dirk Jaeger [1] and Stefan Pelz [2]

[1] Department of Forest Work Science and Engineering, Georg-August-Universität Göttingen, Büsgenweg 4, 37077 Göttingen, Germany; Marta.Paczkowska@uni-goettingen.de (M.P.); Dirk.Jaeger@uni-goettingen.de (D.J.)
[2] Department of Bioenergy, University of Applied Forest Science Rottenburg, Schadenweilerhof, 72108 Rottenburg, Germany; victoriaknappe@gmail.com (V.K.); Pelz@hs-rottenburg.de (S.P.)
[3] Department of Chemical Engineering, University of Santiago de Chile, Avenida Libertador Bernardo, O'Higgins N°3363, Santiago 8320000, Chile; Alonzo.diaz.r@usach.cl
* Correspondence: Sebastian.Paczkowski@uni-goettingen.de; Tel.: +49-7472-951-164

Abstract: The worldwide transformation from fossil fuels to sustainable energy sources will increase the demand for biomass. However, the ash content of many available biomass sources exceeds the limits of national standards. In this study, short-rotation coppice willow biomass was hydrothermally treated at 150, 170 and 185 °C. The higher heating value increased by 2.6% from $\overline{x}$ = 19,279 J × g^{-1} to $\overline{x}$ = 19,793 J × g^{-1} at 185 °C treatment temperature. The mean ash content was reduced by 53% from $\overline{x}$ = 1.97% to $\overline{x}$ = 0.93% at 170 °C treatment temperature, which was below the limit for category TW1b of the European pellet standard for thermally treated biomass. The nitrogen, sulfur and cadmium concentrations were reduced below the limits for category TW1b of the European biomass pellet standard (N: from 0.52% to 0.34%, limit at 0.5%; S: from 0.051% to 0.024%, limit at 0.04%; Cd: from 0.83 mg × kg^{-1} to 0.37 mg × kg^{-1}, limit at 0.5 mg × kg^{-1}). The highest reduction rates were sampled for phosphor (80–84%), potassium (78–90%), chlorine (96–98%) and lithium (96–98%). The reduction behavior of the elements is discussed according to the chemical processes at the onset of hydrothermal carbonization. The results of this study show that HTT has the potential to expand the availability of biomass for the increasing worldwide demand in the future.

Keywords: trace elements; hydrothermal carbonization; biomass; emissions; combustion

Citation: Paczkowski, S.; Knappe, V.; Paczkowska, M.; Diaz Robles, L.A.; Jaeger, D.; Pelz, S. Low-Temperature Hydrothermal Treatment (HTT) Improves the Combustion Properties of Short-Rotation Coppice Willow Wood by Reducing Emission Precursors. *Energies* **2021**, *14*, 8229. https://doi.org/10.3390/en14248229

Academic Editor: Mejdi Jeguirim

Received: 1 November 2021
Accepted: 2 December 2021
Published: 7 December 2021

1. Introduction

There are two water-based processes that can improve the properties of biomass: water leaching and hydrothermal carbonization (HTC).

Water leaching is used in order to dissolve the inorganic fraction of biomass in water [1–6]. This reduces the ash content in the biomass and, therefore, the emission of fine dust particles during combustion. This method has been applied to wood [1,3,4] and other lignocellulose biomasses, e.g., grass or leaves [5]. While the ash content was reduced significantly in these studies, the heating value was not always increased. This contradicted the negative correlation between heating value and ash content [7]. Woody biomass in particular did not show a heating value increase, which was attributed to simultaneous losses of organic matter [1].

Hydrothermal carbonization (HTC) is applied in order to transform biomass into biocoal [8–10]. HTC has been applied to lignocellulose biomass, e.g., straw [1–13], palm fruit bunches [11], sugar cane bagasse [12,13], pine cones [14], pine needles [14], pine wood [13], tahoe wood [13], juniper wood [13], willow wood [15] and eucalypt wood [16], in order to increase its energy density for combustion. The major chemical reactions in the

aqueous environment of the HTC process are hydrolysis, dehydration and decarboxylation. The first reaction mechanism degrades the lignocellulose carbohydrates (hemicellulose, cellulose) by acetal hydrolysis, which yields oligomers and monomers with increased oxygen content [7,17]. Dehydration and decarboxylation deplete these fragments from oxygen and increase the heating value of the biomass. Aromatic compounds are formed, and side reactions yield oxidized organic by-products [18], e.g., acetic, lactic, levulinic, acrylic or formic acid [19–22]. The acid accumulation decreases the pH and increases the ionic product in the liquid phase. Both effects cause a depletion of trace elements from the biomass. In contrast, the reduction of the organic content in the biocoal increases the relative trace element content [17,23–27], which also catalyzes the carbonization at higher temperatures [28].

Many trace elements are combustion emission precursors, and their concentration in the biomass defines its quality. Potassium forms volatile salts, e.g., KCl or K_2SO_4, and K_2CO_3. Chlorine forms volatile salts (KCl or $HgCl_2$ [29]), as well, but it can also form HCl, which causes corrosion in the flue gas pipe [7]. Zinc is an important emission precursor, as it is present in fine dust particles at high concentrations [30–32]. It was sampled with potassium in wood at a ratio of 1:10 [32]. Further inorganic compounds formed in the fire bed at 600 °C are $CaCO_3$ and $K_2Ca(CO_3)_2$, while higher temperatures yield CaO and MgO [33]. Sodium can form $NaSO_4$ and was found in the fire bed and in the fine dust particles at comparably low amounts [32].

The reduction of emission precursors allows biomass to be upgraded for combustion. The element-specific concentrations and the ash content are recommended, e.g., in the European fuel standard DIN EN ISO 17225-2 [34]. The emission limits are regulated, e.g., in the German emission regulation 1.BImSchV [35].

In this study, the possibility of upgrading short-rotation coppice willow biomass by low-temperature hydrothermal treatment (HTT) is evaluated. The process severity of HTT is higher than that of room-temperature water leaching [1–6] and lower than that of HTC [23,26,36]. This study evaluates how the intermediate process parameters of HTT allow the positive effects of water leaching (reduction of trace elements) and HTC (increase in heating value) to be combined, with an emphasis on the specific trace elements that are emission precursors.

2. Materials and Methods

2.1. Sample Material

The willow clone type "Tordes" ((*Salix schwerinii* x *S. viminalis*) x *S. vim.*) was harvested at the age of five with a shredder. The trees were 12–14 m high and had a chest diameter of 15 cm. The flakes were dried (24 h/105 °C) in a kiln dryer of the Schellinger KG (Weingarten, Germany). The dried flakes were cut and ground to wood dust for HTT treatment and subsequent analysis (1 mm sieve, pulverisette 19, Fritsch GmbH, Markt Einersheim, Germany/0.12 mm sieve, ZM 200, Retsch Technology GmbH, Haan, Germany).

2.2. Low-Temperature Hydrothermal Treatment (HTT)

The low-temperature hydrothermal treatment was done in a floor stand Parr reactor (Series 4520, Parr Instrument Company, Moline, IL, USA). The 2000 mL reaction vessel was filled with 140 g of the wood dust and 1400 mL demineralized water. The three applied maximum heat programs were 150 °C (ramp 40 to 150 °C at 2.7 °C × min^{-1}, hold 5 min with maximum pressure 4.7 bar, ramp 150 to 40 °C at −4.8 °C × min^{-1}), 170 °C (ramp 40 to 170 °C at 3.8 °C × min^{-1}, hold 5 min with maximum pressure 8.5 bar, ramp 170 to 40 °C at 3.9 °C × min^{-1}) and 185 °C (ramp 40 to 185 °C at 3.8 °C × min^{-1}, hold 5 min with maximum pressure 12.4 bar, ramp 185 to 40 °C at 3.6 °C × min^{-1}). The reaction vessel was stirred at 200 rpm. Each temperature run was repeated three times. The biocoal was rinsed with distilled water, mechanically pressed in a filter sheet and dried (24 h/105 °C) to prepare for the subsequent analysis.

2.3. Severity Factor

The severity factor of the low-temperature treatment was calculated according to the formula given by Overend et al. and Hoekman et al. [37,38]:

$$Severity\ factor = \lg\left(t \times e^{(T-100)\times 14.75^{-1}}\right) \quad (1)$$

with $t \times e^{(T-100)\times 14.75^{-1}}$ = RO (reaction ordinate) [min]; t = experimental reaction time [min] and T = maximum temperature [°C].

The formula assumes first-order kinetics.

2.4. Ash Content

The determination of the ash content was done by following the procedure in the standard DIN EN ISO 18122:2016-03.

2.5. Heating Value

The higher heating value was measured by following the procedure in the standard DIN EN 14918. The calculation of the lower heating value was done according to DIN 51900-1. In order to prepare an IC analysis, 5 mL of water was pipetted into the bomb of the calorimeter (C6000, IKA-Werke GmbH & Co.KG, Stauffen, Germany).

2.6. Ion Chromatography (IC)

The water added to the calorimeter bomb was used to determine the chlorine and sulphate content. Details of the analysis can be found in [7].

2.7. Elemental Analysis (EA)

Samples of 20 mg each were analyzed. The molar weight shares of C, N and H (varioMACRO cube, elementar Analysesysteme GmbH, Langenselbold, Germany) were calculated according to [7]. The molar oxygen amount was calculated. The results were displayed in form of the O/C and H/C ratio and in the van Krevelen diagram.

2.8. Induced Coupled Plasma-Optical Emission Spectroscopy (ICP-OES)

The trace elements in the samples were analyzed according to EN ISO 1185 with an elemental analyzer (Spectro Blue-EOP-TI ICP-OES, Spectro Analytical Instruments GmbH, Kleve, Germany). The detailed procedure is described in [7].

2.9. Gas Chromatography-Mass Spectrometry (GC-MS)

The HTT process water was filtered with a funnel cellulose filter (150 µm mesh), and then 0.5 mL of it was mixed with 19.5 mL methanol (ratio 1:20). The samples were analyzed according to the procedure described in [7]. An alkane row (C6–C20) was used to calculate the linear retention index to confirm the identity of the detected compounds [39].

2.10. pH of HTC Water

The pH of the filtered HTT process water was sampled (pH 3310, Xylem Analytics Germany Sales GmbH & Co. KG, Weilheim, Germany).

2.11. Statistics

The Shapiro–Wilks test was used to test the datasets for normal distribution. As a consequence, the Steel–Dwass–Critchlow–Fligner procedure for non-normally distributed data was used to identify significant differences between all datasets (each reaction temperature and raw material).

3. Results

3.1. Severity Factor

The severity factor of the highest treatment temperature (185 °C) was four, which indicated the onset of hydrothermal carbonization. The severity factors of the treatments at 150 and 170 °C were below four (2.9 and 3.5, respectively), which indicated the absence of hydrothermal carbonization (Table 1).

Table 1. Data of the calorimetric and elemental analysis of the HTT treatment (mean ± standard deviation (coefficient of variation)). Different letters indicate significant differences of $p < 0.05$ between the datasets.

Treatment	Severity Factor	Ash Content [$\%_{DM}$]	Higher Heating Value [J × g^{-1}]	Lower Heating Value [J × g^{-1}]	C [mmol × g^{-1}]	H [mmol × g^{-1}]	O [mmol × g^{-1}]	H/C	O/C
untreated	-	1.97 ± 0.03 (1.6) A	19,279 ± 62 (0.3) A	17,991 ± 62 (0.3) A	40.9 ± 0.12 (0.3) AB	65.83 ± 0.32 (0.5) A	27.35 ± 0.11 (0.4) A	1.61 ± 0.01 (0.5) A	0.67 ± 0.005 (0.7) A
150 °C	2.9	1.26 ± 0.07 (5.4) B	19,153 ± 108 (0.6) B	17,854 ± 108 (0.6) B	40.69 ± 0.33 (0.8) AB	65.68 ± 0.29 (0.5) A	27.59 ± 0.29 (1.1) A	1.61 ± 0.01 (0.5) A	0.68 ± 0.01 (2.5) A
170 °C	3.5	0.93 ± 0.08 (9.1) C	19,405 ± 143 (0.7) A	18,123 ± 0.8 (0.8) A	40.71 ± 0.17 (0.4) B	63.99 ± 0.36 (0.6) B	27.73 ± 0.14 (0.5) A	1.57 ± 0.01 (0.6) B	0.68 ± 0.01 (0.9) A
185 °C	4.0	0.97 ± 0.06 (5.7) C	19,793 ±64 (0.3) C	18,513 ± 64 (0.3) C	40.99 ± 0.1 (0.3) C	63.76 ± 0.25 (0.4) B	27.51 ± 0.08 (0.3) A	1.56 ± 0.01 (0.3) C	0.67 ± 0.01 (0.6) A

3.2. Ash Content

The ash content was significantly decreased by all treatment temperatures. The ash depletion intensity increased until 170 °C and insignificantly decreased again at 185 °C.

3.3. Heating Value

The heating value significantly dropped at 150 °C and significantly increased again at 185 °C (Table 1).

3.4. Elemental Analysis

The carbon content increased with increasing treatment temperature, while the hydrogen content was reduced. Oxygen showed an insignificant increase from untreated biomass to 170 °C and decreased again to the level of 150 °C at 185 °C (Table 1). The O/C ratio did vary, albeit only slightly, while the H/C ratio was reduced with increasing treatment temperature. This resulted in a vertical downward trend in the van Krevelen diagram and in an undifferentiated horizontal value distribution. A slight shift to the left was observed for the 185 °C treatment (Figure 1).

3.5. Elements and Trace Elements

The elements quantified in this study were reduced at all three treatment temperatures (Table 2). At 150 °C, seven of twelve reductions were significant. At 170 °C, all elements showed a significant reduction in comparison to the untreated biomass. At 185 °C, an increase in nitrogen and sodium caused an insignificant difference from the untreated biomass. The concentrations of sulfur, phosphorous and zinc also increased from 170 to 185 °C, but this did not affect the significant difference from the untreated biomass (Table 2).

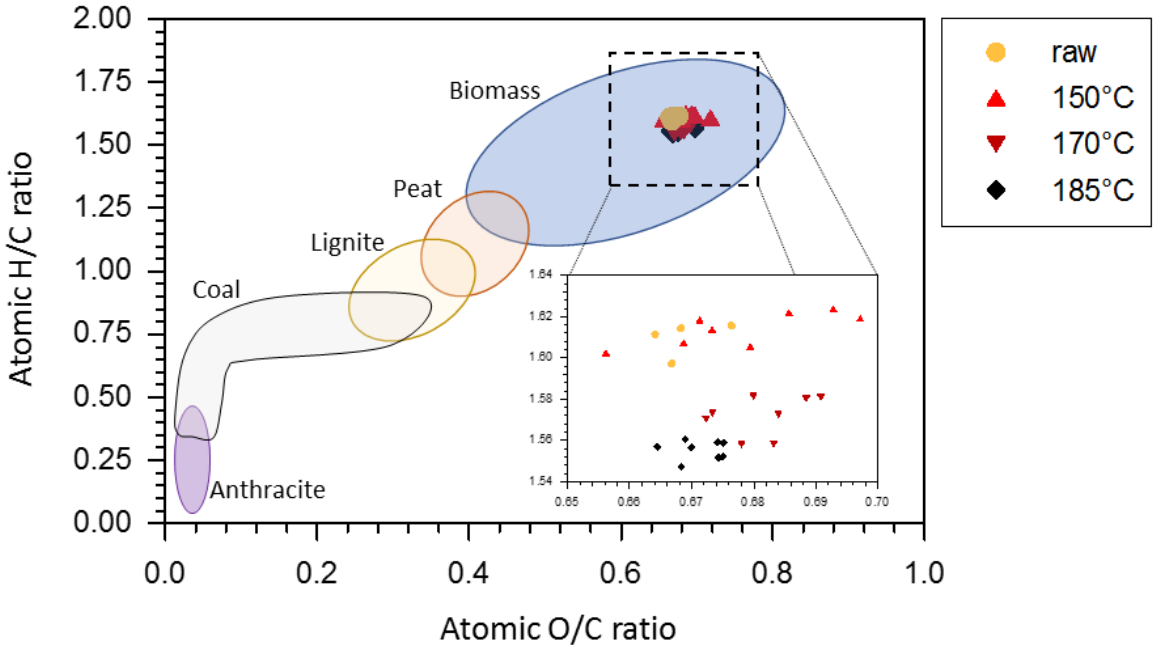

Figure 1. Van Krevelen diagram for the short-rotation coppice (SRC) biomass in comparison to different carbonized materials [19]. The inset shows the depletion of hydrogen and oxygen for the different intensities of the hydrothermal treatment.

Table 2. Elements and trace elements detected in the raw material and the thermally treated material (mean ± standard deviation (coefficient of variation [%])). Different letters indicate significant differences of $p < 0.05$ between the datasets.

Elements	N	S	Cl	P	K	Ca	Mg	Na	Zn	Mn	Cd	Li
						$mg \times kg_{DM}^{-1}$						
Raw	5200 ± 1000 (19) A	516 ± 25 (5) A	58 ± 16 (27) A	955 ± 36 (4) A	2163 ± 96 (4) A	4750 ± 390 (8) A	375 ± 25 (7) A	14 ± 4 (29) A	73 ± 8 (11) A	32 ± 3 (10) A	0.83 ± 0.03 (3.4) A	3.89 ± 2.7 (2.7) A
150 °C	4100 ± 500 (12) AB	271 ± 140 (52) B	4.4 ± 2.7 (63) B	181 ± 22 (12) B	528 ± 48 (9) B	4230 ± 348 (8) A	247 ± 18 (7) B	11 ± 4 (35) A	59 ± 5 (9) A	25 ± 6 (24) A	0.67 ± 0.12 (18) B	0.17 ± 0.05 (28) B
170 °C	3400 ± 400 (11) B	214 ± 153 (71) B	3.4 ± 3.2 (92) B	124 ± 14 (11) C	327 ± 48 (15) C	3151 238 (8) B	115 ± 23 (20) C	7 ± 2 (34) B	40 ± 3 (8) B	11 ± 4 (36) B	0.44 ± 0.05 (10) C	0.17 ± 0.14 (84) BC
185 °C	3600 ± 500 (13) AB	267 ±1 33 (50) C	3.0 ± 1.7 (57) B	132 ± 7 (6) C	242 ± 37 (15) D	2956 ± 109 (4) B	71 ± 7 (10) D	12 ± 3 (25) A	43 ± 9 (20) B	5 ± 1 (17) C	0.37 ± 0.01 (4) D	0.07 ± 0.03 (50) C

The elements in the raw biomass with concentrations in the parts per 1000 range were N, Ka and Ca followed by S, P and Mg in the parts per 10,000 range. Elements with a concentration below the parts per 10,000 range were Cl, Na, Zn, Mn, Cd and Li. The element-specific relative reduction rate did not depend on the absolute concentration of the respective elements (Figure 2, Table 2). The reduction mechanisms of the elements were element-specific. Three types of reduction were observed: 1) high reduction and low difference between temperatures; 2) low reduction with maximum at 185 °C; and 3) low reduction with maximum at 170 °C (Figure 3).

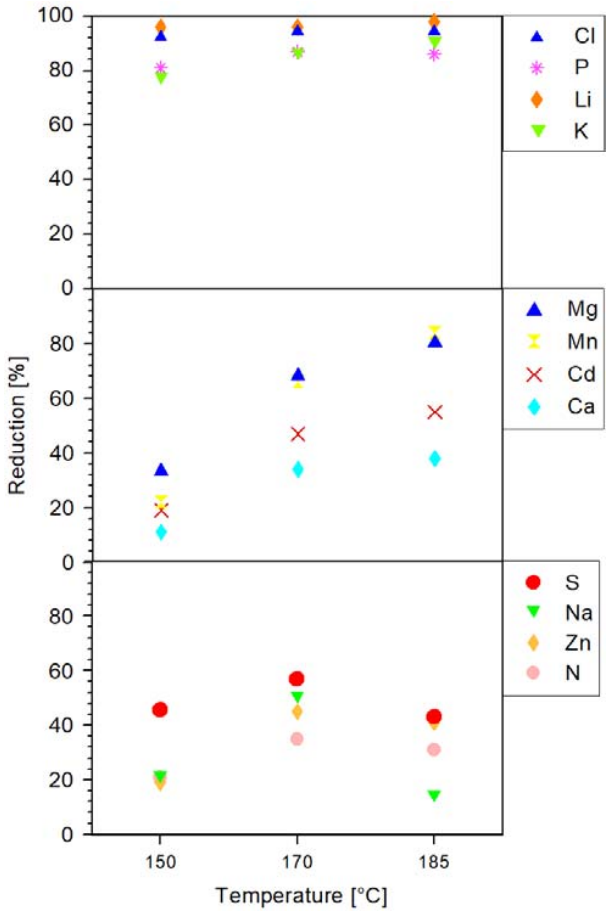

Figure 2. Elements assigned to three different groups according to their leaching behavior.

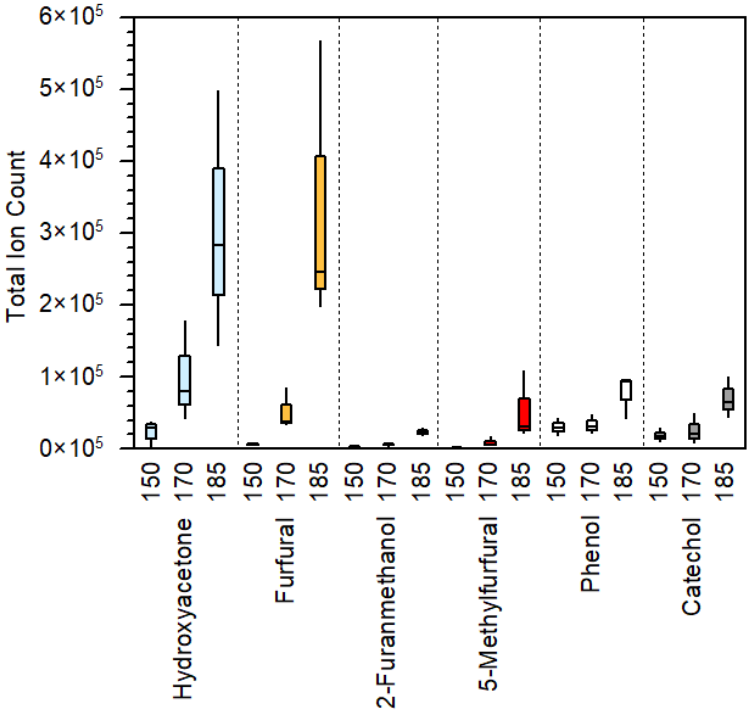

Figure 3. Total ion count (TIC) of the identified substances in the HTT process water at the respective HTT temperatures. The boxplots show the median, lower/upper quartile (box) and minimum/maximum (lines) based on $n = 3$.

3.6. pH

The pH was constantly decreasing with increasing treatment temperature (Table 3).

Table 3. pH of the HTT process water (mean ± standard deviation (coefficient of variation [%])).

Treatment Temperature	pH
150 °C	4.46 ± 0.05 (1.0)
170 °C	4.05 ± 0.03 (0.7)
185 °C	3.94 ± 0.04 (1.1)

3.7. GC-MS Analysis

Six compounds were preliminarily confirmed by the NIST data analysis. Their identity was further confirmed by their retention indices [39]. Among the six compounds were three furans and two benzenes (Table 4). The concentration of all compounds increased with increasing treatment temperature. The increase from 150 to 170 °C was lower than the increase from 170 to 185 °C for all compounds (Figure 3).

Table 4. Identified substances, their respective retention time and retention index on the HP5 column, as well as their CAS number, vapor pressure and water solubility.

Substance	Retention Time [min]	LRI	CAS Number	Vapor Pressure [mmHg at 25 °C]	Solubility in Water [g × L^{-1} at 25 °C]
Hydroxyacetone	6.7	690	116-09-6	1.91	-
Furfural	10.6	830	98-01-1	2.23	77
2-Furanmethanol	11.3	851	98-00-0	1.01	221
5-Methylfurfural	14.8	961	620-02-0	0.64	29
Phenol	15.2	973	108-95-2	0.61	26
Catechol	22.1	1187	120-80-9	0.02	461

4. Discussion

4.1. Heating Value and Elemental Analysis

The higher and lower heating values significantly decreased at 150 °C. This effect was attributed to the acetal hydrolysis of carbohydrates and was also found in a study on low-temperature microwave-assisted hydrothermal carbonization [17,26]. The hydrolysis of the model compound sucrose, for instance, is exothermic:

$$C_{12}H_{22}O_{11} \rightarrow 2C_6H_{12}O_6 \ (\Delta HR; 298 = -4.2 \text{ kJ} \times \text{mol}^{-1}) \quad (2)$$

Therefore, the high share of hemicellulose in willow wood causes a significant drop in the heating value at low temperatures. The acetal hydrolysis also caused an increase in the oxygen level (Table 1 and Figure 1) by recovering the OH- groups in the ester bonds between the sugar molecules. An increase in hydrogen was only detected for three out of eight samples at 150 °C (Figure 1, inset), which were the three samples that also showed the highest O/C ratio at this temperature. Apparently, the acetal hydrolysis only affected these three samples, while the other five samples were not affected and showed values comparable to untreated biomass (Figure 1). This was caused by an uneven heat distribution in the aluminum mantle heat reactor [40], which led to a high result variation within the 150 °C HTT batch.

From 150 to 170 °C, the heating value increased to the level of the raw material, which was due to endothermic reactions, e.g., dehydration. The formation of furfural (Figure 3) from C5 sugars by dehydration, for instance, is endothermic:

$$C_5H_{10}O_5 \rightarrow C_5H_4O_2 + 3H_2O \ (\Delta HR; 298 = 181 \text{ kJ} \times \text{mol}^{-1}) \quad (3)$$

These endothermic reactions were correlated to the significant depletion of hydrogen in the biomass, but not to a significant depletion of oxygen (Table 1, Figure 1, inset). This was an unexpected result, as the dehydration should have decreased the oxygen concentration in the hydrothermally treated biomass significantly. Again, the uneven heat distribution of the 150 °C HTT batch caused this effect. In the inset in Figure 1, a shift from higher O/C and H/C ratios from 150 °C to lower ratios at 170 °C can be observed, considering only the three 150 °C samples that were exposed to intense acetal hydrolysis. Due to the five samples at 150 °C that did show oxygen levels of untreated biomass, the mean gain and loss of oxygen between 150 and 170 °C was almost balanced (Figure 1, inset, Table 1).

The carbonization gained intensity from 170 to 185 °C, (Table 1, Figure 1, inset), and the heating value significantly increased [37,38]. This indicated that condensation reactions and inter- and intramolecular dehydration took place, which was confirmed by increasing concentrations of aromatic compounds in the process water (Figure 3). Also, the variation of the values decreased as shown for the MAHC treatment (Figure 1, inset, [17]). As phenol inhibits polycondensation reactions of aromatic compounds [41], its occurrence in the process water (Figure 3) also explains the low intensity of condensation reactions (Table 1).

4.2. Severity Factor and van Krevelen Diagram

The severity factor of the three applied HTT temperatures was low in this study. This allowed us to gain insights into the early chemical changes of SCR willow wood. According to results shown by Hoekman et al. [37,38], a severity factor below 4.0 is too low to increase the heating value to levels above biomass. This was confirmed in this study, as the mean heating value increase from untreated biomass to 185 °C was only 2.6%. This is also reflected in the van Krevelen diagram, where the O/C and H/C ratios of SRC willow wood are displayed in the context of other carbonized biomass types (Figure 1). All of the applied treatment temperatures caused O/C and H/C ratios above those of peat (Figure 1). The lower variability of the H, C and O values induced by hydrothermal treatment in comparison to untreated biomass was observed by Liu et al. and Knappe et al. [17,26,42]. This variation reduction effect of HTT was also visible at 185 °C in this study (Figure 1, inset). The acids yielded during HTT (Table 3) affected the hydrolysis intensity, as shown by Qi et al. in a study on solid acid-catalyzed corncob hydrolysis [43].

4.3. Trace Element Behavior

4.3.1. Nitrogen and Sulfur

Nitrogen is a major element in the backbone of proteins and in the DNA, while sulfur is present in the amino acids methionine and cysteine. When the organic polymers in the willow wood tissue are thermally degraded, both elements are converted to sulfite, sulfide, nitrite and nitrate anions [44]. This explains their low reduction rate at 150 °C, because at this temperature the organic tissue is not degraded at high rates (Table 1). In solution, the elements can bind to cations and form, e.g., Li_2SO_3, $MgSO_3$, K_2SO_3, Na_2SO_3, $CaSO_3$ and $ZnSO_3$ or the respective sulfates. Sulfites and sulfates have a low solubility in water due to their basic nature. The acidic environment of the HTT liquid phase improves their solubility, which explains their increasing depletion (Table 2).

An increasing ionic product caused by the temperature increase in the reactor (Table 3) can precipitate sulfites and sulfates to the solid phase. The ionic product still increased at 185 °C (Table 1, ash content, and Table 2), while the pH was almost constant (Table 3). This can explain the reduced reduction of sulfur and nitrogen at 185 °C (Figure 2). Another reason for this reduced reduction can be aromatic sulfonation or nitration at relatively low temperatures, which occurs under acid conditions [43]. The increase in the heating value due to aromatic compound formation occurred at 185 °C (Table 1). The reintegration of sulfur and nitrogen in these compounds can explain the decrease in the reduction rate at 185 °C, as well. The low depletion rate of sulfur and nitrogen in many HTC studies confirms their reintegration in the solid phase at higher treatment temperatures [11,13,24,45,46].

4.3.2. Phosphor

Phosphor was significantly reduced (Table 2, Figure 2). It is present in biomass in water-soluble compounds, e.g., ATP (50 mg × mL^{-1}) and DNA (20 mg × mL^{-1}). Phosphate salts have a low solubility in water and are precipitated at high ion concentrations. Therefore, the high depletion rate in comparison to sulfur and nitrogen suggests that phosphor compounds were not degraded at HTT temperatures, but directly solved in the water phase. During combustion, phosphor salts are formed and remain in the fire bed without contributing to fine dust formation [32].

4.3.3. Chlorine

The anion chlorine was present at a comparably low concentration (Table 2). Chlorine forms strong electrolyte salt ions with high solubility in water. KCl and LiCl are increasingly soluble at increasing temperatures. Both explain the assignment of chlorine to group 1 in Figure 2. The salts KCl and NaCl are formed predominantly. The high solubility of chlorine was confirmed by studies on room-temperature water leaching [4,5].

4.3.4. Calcium and Magnesium

The cations Ca and Mg were assigned to group 2 (Figure 2). Their solubility under HTC conditions depends on the formation of acetic acid and nitrite/nitrate. These anions form calcium and magnesium salts. Sulfur anions cause a very low solubility of these salts. Chlorine is a potential anion for Ca and Mg, but could not influence the Mg and Ca depletion due to its low abundance in the biomass (Table 2). Calcium and magnesium oxides remain in the fire bed and only slightly contribute to fine dust formation [32], while they are important factors for ash slagging [47].

4.3.5. Sodium

Sodium showed a much less intense solubilization in comparison to potassium and chlorine (Figure 2), although all three elements are strong electrolytic salts with high water solubility. The solubility of the sodium salts NaCl, Na_2SO_x and CH_3COONa does not increase at higher temperatures. Therefore, sodium shows a highly variable temperature-dependent reduction rate (Figure 2).

4.3.6. Zinc

Zinc had a low concentration in the untreated biomass and was reduced only by 19–46% due to its low solubility and restricted salt formation capability. Possible anions are, e.g., chloride, nitrite/nitrate or sulfite/sulfate anions. Zinc can also form complexes with aromatic structures, e.g., porphyrins. This can explain its assignment to group 3 in Figure 3. The onset of aromatic ring formation can lead to a chelatization of zinc in the solid phase and, thereby, reduce its reduction rate.

The vapor pressure of zinc is very low, but its oxidation to ZnO leads to an increase in vapor pressure. As a consequence, the compound is emitted to the gaseous phase in the combustion unit. There it condenses in the upper flue gas pipe zones at low temperature and serves as a nucleation agent for potassium salts and other volatile salts [48]. Due to this effect, zinc is an important fine dust precursor.

4.3.7. Lithium

Lithium was reduced by 96–98% due to its high solubility in water. The element readily forms soluble salts with almost all anions and is highly reactive. Therefore, it showed the highest reduction rates in this study.

4.3.8. Cadmium

Cadmium can form complexes with zinc. It can also yield water-soluble salts with Cl_2, SO_4, CO_3, S and organic acids [49], which explains why the solubility of cadmium (group 2) is not complementary to the zinc concentration (group 3) (Figure 3).

4.3.9. Manganese

Manganese can form water-soluble salts with the anions nitrite/nitrate, chlorate and sulfite/sulfate. It can oxidize in water and gain various oxidation states, which decreases its capability to form salts. The oxides, however, are still water-soluble and can even react with water to form manganese hydroxide. Manganese showed the highest relative increase in the leaching rate (Figure 3), which indicates a temperature-dependent mechanism of its solubility in water.

4.4. Comparison of HTT and MAHC

Microwaves can penetrate the reactor volume better than infrared radiation and, therefore, can heat the water/biomass mixture more evenly. This led to a reduced result variation in the respective MAHC study in comparison to this study [38,39].

The heating value of both treatments confirmed the higher conversion efficiency of the MAHC. The microwaves increased the higher heating value to 20,029 J $\times$ g^{-1}, while in this study the maximum mean was 19,793 J $\times$ g^{-1}. The discussed hydrolysis-induced heating value drop at 150 °C was visible in both studies, though the variability in the van Krevelen diagram was higher in this study.

The mean ash content of the MAHC biomass treatment increased from 0.9% (170 °C) to 1% (185 °C), while the mean ash content in this study increased from 0.93% (170 °C) to 0.97% (185 °C) in the same temperature range. This was caused by the higher carbonization intensity of the MAHC. Therefore, the mean depletion of oxygen was higher during the MAHC treatment (raw: 29.04 µmol $\times$ g^{-1}; 185 °C: 27.94 µmol $\times$ g^{-1}, significant difference) in comparison to the HTT (raw: 27.35 µmol $\times$ g^{-1}; 185 °C: 27.51 µmol $\times$ g^{-1}, slight increase). Also, the variation of the C, O and H concentrations was already reduced at 150 °C, while in this study the effect occurred at 185 °C [17].

Elements with the same reduction in both studies were calcium and potassium. Magnesium showed the same trend, but with a much higher reduction rate in the MAHC study, which could be explained by the lower pH in the MAHC study that favored the formation of magnesium acetate salts. $Mg(C_2H_3O_2)_2$ is the salt with the highest solubility of magnesium salts that can be formed during biomass HTC/HTT. The solution of calcium acetates in water is not temperature-dependent; therefore, a higher depletion of calcium is not probable due to the lower pH. Sodium and zinc reduction constantly increased in the MAHC study, while in this study both compounds showed an increased reduction rate from 150 to 170 °C and decreased reduction rate from 170 to 185 °C. This indicates that the solubility reduction of sodium and zinc was restricted to a short interval in the succession of carbonization reactions.

The comparative analysis of the two laboratory-scale studies confirmed the higher reaction intensity of the MAHC treatment. However, industrial-scale MAHC is more expensive than a conventional batch or continuous reactor. Therefore, biocoal production is only performed with conventional reactors in industry. HTT can be upscaled with conventional reactors to produce large quantities of upgraded biomass for sustainable heat and electricity production. Another advantage of HTT treatment is the comparably low concentration of aromatic compounds in the process water, which can be used as fertilizer according to national regulations.

5. Conclusions

Hydrothermal treatment (HTT) in a conventional pressure reactor is a feasible method to improve the combustion properties of biomass. In this study, the ash content was significantly decreased, and all of the analyzed elements were reduced. Among them were important emission precursors such as nitrogen, potassium, chlorine and zinc. The reduction of the ash content is a major advantage of HTT over HTC, where the ash content increases due to the reduction of the organic fraction [17,23–27].

The heating value of the biomass increased significantly with increasing temperature, with a significant drop at 150 °C. This drop was attributed to the exothermal acetal hy-

drolysis of hemicellulose. At higher treatment temperatures (170 and 185 °C), the heating value increased and the high variation of the O/C and H/C ratios, which was an effect of the uneven heat distribution in the reactor, was superimposed by the carbonization reactions. The increase in the heating value due to ash reduction and carbonization is an advantage over water leaching, where the heating value is not or only slightly affected by the ash reduction in the case of woody biomass [1]. For grass and foliage, an LHV increase of up to 10% was reported after water leaching. On the other hand, the concentration of the emission precursor zinc increased by 30–54%, which is a major drawback of the water leaching method [5].

Both the ash content reduction and the heating value increase proved that HTT combines the positive effects of room-temperature water leaching and HTC in this study. Therefore, HTT can be recommended for wood biomass fuel upgrading. The reduction intensity of the elements followed complex inorganic and organic interactions between solid and liquid phase.

An application of HTT for upgrading wood biomass for combustion requires an external heat source, because exothermal reactions are not intense at HTT temperatures. The process water contained plant nutrients and can be upgraded to a fertilizer by extracting the comparably low aromatic compound load. This water-based aromatic compound extract with, e.g., furans and phenols, can be sold to the chemical industry as a pre-fraction for further purification.

Author Contributions: Conceptualization, S.P. (Sebastian Paczkowski), S.P. (Stefan Pelz) and V.K..; methodology, S.P. (Sebastian Paczkowski), V.K., M.P.; validation, S.P. (Sebastian Paczkowski), D.J., S.P. (Stefan Pelz); resources, L.A.D.R., S.P. (Stefan Pelz), D.J.; data curation, S.P. (Stefan Pelz), M.P., V.K.; writing—original draft preparation, S.P. (Sebastian Paczkowski), V.K.; writing—review and editing, S.P. (Sebastian Paczkowski), D.J., L.A.D.R., S.P. (Stefan Pelz); visualization, S.P. (Sebastian Paczkowski), M.P., V.K.; supervision, L.A.D.R., D.J., S.P. (Stefan Pelz); project administration, L.A.D.R., S.P. (Sebastian Paczkowski), S.P. (Stefan Pelz); funding acquisition, L.A.D.R., S.P. (Stefan Pelz). All authors have read and agreed to the published version of the manuscript.

Funding: This research was funded by the BMBF, Bundesministerium für Bildung und Forschung, grant number 01DN16036.

Institutional Review Board Statement: Not applicable.

Informed Consent Statement: Not applicable.

Data Availability Statement: The data presented in this study are available on request from the corresponding author.

Acknowledgments: The authors thank Rainer Kirchhof, Peter Grammer and Carola Lepski for their technical support.

Conflicts of Interest: The authors declare no conflict of interest.

References

1. Yu, C.; Thy, P.; Wang, L.; Anderson, S.N.; VanderGheynst, J.S.; Upadhyaya, S.K.; Jenkins, B.M. Influence of leaching pretreatment on fuel properties of biomass. *Fuel Process. Technol.* **2014**, *128*, 43–53. [CrossRef]
2. Turn, S.Q.; Kinoshita, C.M.; Ishimura, D.M. Removal of inorganic constituents of biomass feedstocks by mechanical dewatering and leaching. *Biomass Bioenergy* **1997**, *12*, 241–252. [CrossRef]
3. Saddawi, A.; Jones, J.M.; Williams, A.; Le Coeur, C. Commodity Fuels from Biomass through Pretreatment and Torrefaction: Effects of Mineral Content on Torrefied Fuel Characteristics and Quality. *Energy Fuels* **2012**, *26*, 6466–6474. [CrossRef]
4. Liaw, S.B.; Wu, H. Leaching Characteristics of Organic and Inorganic Matter from Biomass by Water: Differences between Batch and Semi-continuous Operations. *Ind. Eng. Chem. Res.* **2013**, *52*, 4280–4289. [CrossRef]
5. Khalsa, J.; Döhling, F.; Berger, F. Foliage and Grass as Fuel Pellets–Small Scale Combustion of Washed and Mechanically Leached Biomass. *Energies* **2016**, *9*, 361. [CrossRef]
6. Gong, S.-H.; Im, H.-S.; Um, M.; Lee, H.-W.; Lee, J.-W. Enhancement of waste biomass fuel properties by sequential leaching and wet torrefaction. *Fuel* **2019**, *239*, 693–700. [CrossRef]
7. Kaltschmitt, M.; Hartmann, H.; Hofbauer, H. *Energie aus Biomasse: Grundlagen, Techniken und Verfahren*, 3rd ed.; Springer: Berlin/Heidelberg, Germany, 2016.

8. Azzaz, A.A.; Khiari, B.; Jellali, S.; Ghimbeu, C.M.; Jeguirim, M. Hydrochars production, characterization and application for wastewater treatment: A review. *Renew. Sustain. Energy Rev.* **2020**, *127*, 109882. [CrossRef]
9. Siwal, S.S.; Zhang, Q.; Devi, N.; Saini, A.K.; Saini, V.; Pareek, B.; Gaidukovs, S.; Thakur, V.K. Recovery processes of sustainable energy using different biomass and wastes. *Renew. Sustain. Energy Rev.* **2021**, *150*, 111483. [CrossRef]
10. Khiari, B.; Jeguirim, M.; Limousy, L.; Bennici, S. Biomass derived chars for energy applications. *Renew. Sustain. Energy Rev.* **2019**, *108*, 253–273. [CrossRef]
11. Parshetti, G.K.; Kent Hoekman, S.; Balasubramanian, R. Chemical, structural and combustion characteristics of carbonaceous products obtained by hydrothermal carbonization of palm empty fruit bunches. *Bioresour. Technol.* **2013**, *135*, 683–689. [CrossRef]
12. Chen, W.-H.; Ye, S.-C.; Sheen, H.-K. Hydrothermal carbonization of sugarcane bagasse via wet torrefaction in association with microwave heating. *Bioresour. Technol.* **2012**, *118*, 195–203. [CrossRef]
13. Hoekman, S.K.; Broch, A.; Robbins, C.; Zielinska, B.; Felix, L. Hydrothermal carbonization (HTC) of selected woody and herbaceous biomass feedstocks. *Biomass Conv. Bioref.* **2013**, *3*, 113–126. [CrossRef]
14. Titirici, M.M.; Thomas, A.; Yu, S.-H.; Müller, J.-O.; Antonietti, M. A Direct Synthesis of Mesoporous Carbons with Bicontinuous Pore Morphology from Crude Plant Material by Hydrothermal Carbonization. *Chem. Mater.* **2007**, *19*, 4205–4212. [CrossRef]
15. Hashaikeh, R.; Fang, Z.; Butler, I.S.; Hawari, J.; Kozinski, J.A. Hydrothermal dissolution of willow in hot compressed water as a model for biomass conversion. *Fuel* **2007**, *86*, 1614–1622. [CrossRef]
16. Garotte, H.; Domingues, H.; Parajo, J.C. Study on the deacetylation of hemicellulose during the hydrothermal processing of Eucalyptus wood. *Holz Roh-und Werkst.* **2001**, *59*, 53–59. [CrossRef]
17. Knappe, V.; Paczkowski, S.; Tejada, J.; Diaz Robles, L.A.; Gonzales, A.; Pelz, S. Low temperature microwave assisted hydrothermal carbonization (MAHC) reduces combustion emission precursors in short rotation coppice willow wood. *J. Anal. Appl. Pyrol.* **2018**, *134*, 162–166. [CrossRef]
18. Sevilla, M.; Fuertes, A.B. The production of carbon materials by hydrothermal carbonization of cellulose. *Carbon* **2009**, *47*, 2281–2289. [CrossRef]
19. Reza, M.T.; Uddin, M.H.; Lynam, J.G.; Hoekman, S.K.; Coronella, C.J. Hydrothermal carbonization of loblolly pine: Reaction chemistry and water balance. *Biomass Conv. Bioref.* **2014**, *4*, 311–321. [CrossRef]
20. Funke, A.; Ziegler, F. Hydrothermal carbonization of biomass: A summary and discussion of chemical mechanisms for process engineering. *Biofuel. Bioprod. Bioref.* **2010**, *4*, 160–177. [CrossRef]
21. Kruse, A.; Dahmen, N. Hydrothermal biomass conversion: Quo vadis? *J. Supercrit. Fluids* **2018**, *134*, 114–123. [CrossRef]
22. Kruse, A.; Funke, A.; Titirici, M.-M. Hydrothermal conversion of biomass to fuels and energetic materials. *Curr. Opin. Chem. Biol.* **2013**, *17*, 515–521. [CrossRef]
23. Reza, M.T.; Lynam, J.G.; Uddin, M.H.; Coronella, C.J. Hydrothermal carbonization: Fate of inorganics. *Biomass Bioenergy* **2013**, *49*, 86–94. [CrossRef]
24. Poerschmann, J.; Weiner, B.; Wedwitschka, H.; Baskyr, I.; Koehler, R.; Kopinke, F.-D. Characterization of biocoals and dissolved organic matter phases obtained upon hydrothermal carbonization of brewer's spent grain. *Bioresour. Technol.* **2014**, *164*, 162–169. [CrossRef]
25. Poerschmann, J.; Weiner, B.; Wedwitschka, H.; Zehnsdorf, A.; Koehler, R.; Kopinke, F.-D. Characterization of biochars and dissolved organic matter phases obtained upon hydrothermal carbonization of Elodea nuttallii. *Bioresour. Technol.* **2015**, *189*, 145–153. [CrossRef] [PubMed]
26. Knappe, V.; Paczkowski, S.; Diaz Robles, L.A.; Gonzales, A.; Pelz, S. Reducing Willow Wood Fuel Emission by Low Temperature Microwave Assisted Hydrothermal Carbonization. *J. Vis. Exp.* **2019**, *147*, e58970. [CrossRef] [PubMed]
27. Liu, Z.; Balasubramanian, R. Upgrading of waste biomass by hydrothermal carbonization (HTC) and low temperature pyrolysis (LTP): A comparative evaluation. *Appl. Energy* **2014**, *114*, 857–864. [CrossRef]
28. Zhou, L.; Zhang, G.; Reinmöller, M.; Meyer, B. Effect of inherent mineral matter on the co-pyrolysis of highly reactive brown coal and wheat straw. *Fuel* **2019**, *239*, 1194–1203. [CrossRef]
29. Senior, C.L.; Helble, J.J.; Sarofim, A.F. Emissions of mercury, trace elements, and fine particles from stationary combustion sources. *Fuel Proc. Technol.* **2000**, *65*, 263–288. [CrossRef]
30. Obaidullah, M.; Bram, S.; Verma, V.K.; De Ruyck, J. A review on particle emissions from small scale biomass combustion. *Int. J. Renew. Energy Res.* **2012**, 147–159.
31. Wiinikka, H.; Gebart, R.; Boman, C.; Boström, D.; Nordin, A.; Öhman, M. High-temperature aerosol formation in wood pellets flames: Spatially resolved measurements. *Combust. Flame* **2006**, *147*, 278–293. [CrossRef]
32. Gehrig, M.; Jaeger, D.; Pelz, S.K.; Weissinger, A.; Groll, A.; Thorwarth, H.; Haslinger, W. Influence of firebed temperature on inorganic particle emissions in a residential wood pellet boiler. *Atmos. Environ.* **2016**, *136*, 61–67. [CrossRef]
33. Misra, M.K.; Ragland, K.W.; Baker, A.J. Wood ash composition as a function of furnace temperature. *Biomass Bioenergy* **1993**, *4*, 103–116. [CrossRef]
34. DIN Normenausschuss Materialprüfung. *Biogene Festbrennstoffe—Brennstoffspezifikationen und-Klassen—Teil 2: Klassifizierung Von Holzpellets*; Beuth: Berlin, Germany, 2014; pp. 1–13.
35. Bundesministerium der Justiz und für Verbraucherschutz. *Erste Verordnung Zur Durchführung des Bundes-Immissionsschutzgesetzes (Verordnung über Kleine und Mittlere Feuerungsanlagen—1. BImSchV)*; Bundesministerium der Justiz und für Verbraucherschutz: Berlin, Germany, 2010.

36. Zhang, D.; Wang, F.; Shen, X.; Yi, W.; Li, Z.; Li, Y.; Tian, C. Comparison study on fuel properties of hydrochars produced from corn stalk and corn stalk digestate. *Energy* **2018**, *165*, 527–536. [CrossRef]
37. Overend, R.P.; Chornet, E.; Gascoigne, J.A. Fractionation of Lignocellulosics by Steam-Aqueous Pretreatments [and Discussion]. *Philos. Trans. R. Soc. Lond. Ser. A* **1987**, *321*, 523–536.
38. Hoekman, S.K.; Broch, A.; Felix, L.; Farthing, W. Hydrothermal carbonization (HTC) of loblolly pine using a continuous, reactive twin-screw extruder. *Energy Convers. Manag.* **2017**, *134*, 247–259. [CrossRef]
39. Castello, G.; Moretti, P.; Vezzani, S. Retention models for programmed gas chromatography. *J. Chromatogr. A* **2009**, *1216*, 1607–1623. [CrossRef] [PubMed]
40. Möller, M.; Harnisch, F.; Schröder, U. Microwave-assisted hydrothermal degradation of fructose and glucose in subcritical water. *Biomass Bioenergy* **2012**, *39*, 389–398. [CrossRef]
41. Zhen, X.; Li, H.; Xu, Z.; Wang, Q.; Xu, J.; Zhu, S.; Wang, Z.; Yuan, Z. Demethylation, phenolation, and depolymerization of lignin for the synthesis of lignin-based epoxy resin via a one-pot strategy. *Ind. Crop. Prod.* **2021**, *173*, 114135. [CrossRef]
42. Liu, Z.; Quek, A.; Balasubramanian, R. Preparation and characterization of fuel pellets from woody biomass, agro-residues and their corresponding hydrochars. *Appl. Energy* **2014**, *113*, 1315–1322. [CrossRef]
43. Qi, W.; Liu, G.; He, C.; Liu, S.; Lu, S.; Yue, J.; Wang, Q.; Wang, Z.; Yuan, Z.; Hu, J. An efficient magnetic carbon-based solid acid treatment for corncob saccharification with high selectivity for xylose and enhanced enzymatic digestibility. *Green Chem.* **2019**, *21*, 1292–1304. [CrossRef]
44. Nizamuddin, S.; Baloch, H.A.; Siddiqui, M.T.H.; Mubarak, N.M.; Tunio, M.M.; Bhutto, A.W.; Jatoi, A.S.; Griffin, G.J.; Srinivasan, M.P. An overview of microwave hydrothermal carbonization and microwave pyrolysis of biomass. *Rev. Environ. Sci. Biotechnol.* **2018**, *17*, 813–837. [CrossRef]
45. Toptas Tag, A.; Duman, G.; Yanik, J. Influences of feedstock type and process variables on hydrochar properties. *Bioresour. Technol.* **2017**, *250*, 337–344. [CrossRef] [PubMed]
46. Xiao, L.-P.; Shi, Z.-J.; Xu, F.; Sun, R.-C. Hydrothermal carbonization of lignocellulosic biomass. *Bioresour. Technol.* **2012**, *118*, 619–623. [CrossRef] [PubMed]
47. Shi, W.; Laabs, M.; Reinmöller, M.; Bai, J.; Guhl, S.; Kong, L.; Li, H.; Meyer, B.; Li, W. In-situ analysis of the effect of CaO/Fe_2O_3 addition on ash melting and sintering behavior for slagging-type applications. *Fuel* **2021**, *285*, 119090. [CrossRef]
48. Sippula, O. Fine Particle Formation and Emissions in Biomass Combustion. Ph.D. Thesis, University of Eastern Finland, Kuopio, Finland, 2010.
49. Lederkremer, R.M.; Marino, C. Acids and other products of oxidation of sugars. *Adv. Carbohyd. Chem. Biochem.* **2003**, *58*, 199–306. [CrossRef]